Analyzing speckle contrast for HiLo microscopy optimization

J. Mazzaferri,[1,2,#] D. Kunik,[1,2,#] J. M. Belisle,[1,2] K. Singh,[1,3] S. Lefrançois,[1,4] and S. Costantino[1,2,5,*]

[1]*Centre de Recherche de l'Hôpital Maisonneuve-Rosemont, Canada*
[2]*Institut de Génie Biomédicale, Université de Montréal, Montréal, QC, Canada*
[3]*Institut National de la Recherche Scientifique, Energie Materiaux et Communications, Varennes, QC, Canada*
[4]*Département de Médecine, Université de Montréal, Montréal, QC, Canada*
[5]*Département d'Ophtalmologie, Université de Montréal, Montréal, QC, Canada*
[#]*These authors contributed equally to this work.*
[*]*santiago.costantino@umontreal.ca*

Abstract: HiLo microscopy is a recently developed technique that provides both optical sectioning and fast imaging with a simple implementation and at a very low cost. The methodology combines widefield and speckled illumination images to obtain one optically sectioned image. Hence, the characteristics of such speckle illumination ultimately determine the quality of HiLo images and the overall performance of the method. In this work, we study how speckle contrast influence local variations of fluorescence intensity and brightness profiles of thick samples. We present this article as a guide to adjust the parameters of the system for optimizing the capabilities of this novel technology.

OCIS codes: (170.6900) Three-dimensional microscopy; (180.2520) Fluorescence microscopy; (110.6150) Speckle imaging; (170.1790) Confocal microscopy.

References and links

1. D. Lim, K. K. Chu, and J. Mertz, "Wide-field fluorescence sectioning with hybrid speckle and uniform-illumination microscopy," Opt. Lett. **33**(16), 1819–1821 (2008).
2. C. Ventalon, R. Heintzmann, and J. Mertz, "Dynamic speckle illumination microscopy with wavelet prefiltering," Opt. Lett. **32**(11), 1417–1419 (2007).
3. D. Lim, T. N. Ford, K. K. Chu, and J. Mertz, "Optically sectioned in vivo imaging with speckle illumination HiLo microscopy," J. Biomed. Opt. **16**(1), 016014 (2011).
4. J. Mertz and J. Kim, "Scanning light-sheet microscopy in the whole mouse brain with HiLo background rejection," J. Biomed. Opt. **15**(1), 016027 (2010).
5. S. Santos, K. K. Chu, D. Lim, N. Bozinovic, T. N. Ford, C. Hourtoule, A. C. Bartoo, S. K. Singh, and J. Mertz, "Optically sectioned fluorescence endomicroscopy with hybrid-illumination imaging through a flexible fiber bundle," J. Biomed. Opt. **14**(3), 030502 (2009).
6. J. W. Goodman, *Introduction to Fourier Optics* (2nd Ed., McGraw-Hill, 1996), Chap. 6.
7. C. Ventalon and J. Mertz, "Quasi-confocal fluorescence sectioning with dynamic speckle illumination," Opt. Lett. **30**(24), 3350–3352 (2005).
8. D. D. Duncan, S. J. Kirkpatrick, and R. K. Wang, "Statistics of local speckle contrast," J. Opt. Soc. Am. A **25**(1), 9–15 (2008).
9. J. Goodman, *Speckle phenomena in optics* (Roberts & Company, 2007).
10. J. M. Bélisle, J. P. Correia, P. W. Wiseman, T. E. Kennedy, and S. Costantino, "Patterning protein concentration using laser-assisted adsorption by photobleaching, LAPAP," Lab Chip **8**(12), 2164–2167 (2008).
11. J. M. Belisle, D. Kunik, and S. Costantino, "Rapid multicomponent optical protein patterning," Lab Chip **9**(24), 3580–3585 (2009).
12. K. Singh, C. Dion, S. Costantino, M. Wajszilber, M. R. Lesk, and T. Ozaki, "Development of a novel instrument to measure the pulsatile movement of ocular tissues," Exp. Eye Res. **91**(1), 63–68 (2010).
13. K. Singh, C. Dion, M. R. Lesk, T. Ozaki, and S. Costantino, "Spectral-domain phase microscopy with improved sensitivity using two-dimensional detector arrays," Rev. Sci. Instrum. **82**(2), 023706 (2011).

#148475 - $15.00 USD Received 1 Jun 2011; revised 30 Jun 2011; accepted 5 Jul 2011; published 13 Jul 2011

1. Introduction

HiLo is a novel fluorescence microscopy modality that provides both optical sectioning and fast imaging at a very low cost. A HiLo microscope can be built with simple modifications to a wide-field illumination setup and does not require complex automation nor sophisticated optomechanical components. As opposed to laser scanning microscopes, optical sectioning is obtained combining two images, one obtained with wide-field illumination and a second one using speckle pattern illumination. This required combination of two images makes the sampling frequency only two times slower than the camera acquisition rate, what is typically one order of magnitude faster than a standard confocal microscope. In addition, since only a coherent light source must be added to a standard fluorescence microscope, the cost of HiLo microscopes is approximately ten times lower than a laser-scanning configuration. The remarkable capabilities of HiLo microscopy have been demonstrated so far using pollen grains, brain slices, zebrafish and worms [1–3], and the width of the optical sections obtained using a 488nm laser are as thin as 1.6μm [1,2]. Furthermore, the basic concept of HiLo can also be used for light-sheet microscopy and fluorescence endoscopies [4,5].

When HiLo microscopy is used for quantitative studies, an in-depth comprehension of the methodology is important for accurate interpretation of images. Artifacts due to speckle pattern illumination may affect brightness, particle density measurements and the computation of sample thickness. Here we present a study describing the types of samples that are suitable for this approach, we experimentally quantify artifacts that arise due to speckle illumination and we provide recipes to possibly overcome them. We present this work as a guide to profit from this novel microscopy, and to understand how certain features of the illumination profile and the sample characteristics render HiLo images that can be difficult to comprehend.

2. HiLo microscopy basics

HiLo microscopy requires two images to obtain one optically sectioned image. A uniform-illumination image (i_u) is used to obtain the high-frequency (HI) components by means of a digital high-pass filter and a second image (i_s), obtained with speckle-illumination, is used to identify the axially resolved low-frequency (LO) components of the object. The combination of these two images provides a full-frequency axially sectioned image.

Optical sectioning in HiLo microscopy is obtained by processing the HI and LO regions of the spatial spectrum of the object in different ways. The procedure used to retrieve the HI in-focus components is based on typical properties of the optical transfer function (OTF) of a standard wide-field microscope. HI components of an object are well resolved only when the object is in focus, while LO components remain visible even if it is out of focus [6]. Therefore, HI components are naturally optically sectioned and they can be extracted from i_u simply using a high-pass Fourier filter (*HP*). The in-focus HI components (i_{hi}) are obtained as $i_{hi}(\vec{\rho}) = \Im^{-1}\{I_u(\vec{\kappa}) \times HP(\vec{\kappa})\}$, where $\Im^{-1}\{\ \}$ stands for the inverse Fourier transform operation, I_u is the Fourier transform of i_u, ρ are spatial coordinates of the image and *HP* is a Gaussian high-pass filter with cutoff frequency κ_c, such that $HP(\vec{\kappa}) = 1/2$ for all $|\vec{\kappa}| = \kappa_c$.

In order to retrieve the in-focus LO components, a speckle pattern is used to illuminate the sample [1,7]. The OTF of the microscope determines that small details of the illumination (high frequency components) yield high image contrast only if they are originated in the in-focus plane of the object; namely an optical section. The speckled epi-fluorescence from all out-of-focus sections present low image contrast. Hence, only the regions of the image that show high speckle contrast correspond to the in-focus axial plane, the rest is out-of-focus background. Therefore, the contrast in i_s is an indicator of in-focus information, which is calculated locally within square sampling windows of side Λ throughout the image, according to

#148475 - $15.00 USD Received 1 Jun 2011; revised 30 Jun 2011; accepted 5 Jul 2011; published 13 Jul 2011

$$C_S(\vec{\rho}) = \frac{\langle \sigma_S \rangle_\Lambda}{\langle i_S \rangle_\Lambda}, \tag{1}$$

where $\langle \sigma_S \rangle_\Lambda$ and $\langle i_S \rangle_\Lambda$ are the standard deviation and the mean value of i_s respectively, computed locally within each sampling window. Since only the intensity variations caused by speckle are sought, C_S should be corrected to eliminate the variations due to the object itself [1]. An alternative approach consists on calculating the local contrast on the image difference i_s-i_u, as it was recently proposed [3]. Finally, C_S is applied as a weighting function on i_u to obtain

$$i_{su}(\vec{\rho}) = C_S(\vec{\rho}) \times i_u(\vec{\rho}), \tag{2}$$

which is a low-resolution image of the in-focus plane of the object. In order to obtain the LO components of the object that belong only to a frequency range that is complementary to i_{hi}, a complementary low-pass filter *LP = 1 - HP* is applied as $i_{lo}(\vec{\rho}) = \Im^{-1}\{I_{su}(\vec{\kappa}) \times LP(\vec{\kappa})\}$, where I_{su} is the Fourier transform of i_{su}. The final image, containing the in-focus information of the full spatial frequency range, is computed as $i_{HiLo}(\vec{\rho}) = \eta \times i_{lo}(\vec{\rho}) + i_{hi}(\vec{\rho})$, where the parameter η balances both intensities for avoiding discontinuities at κ_c in the spatial spectrum of i_{HiLo} [1, 3].

It should be noted that the size of the window used to calculate C_s determines the sampling of i_{su}. Therefore, the maximum spatial frequency component that is present in i_{su} is $1/2\Lambda$ and in order to obtain the full spatial spectrum of the object, the cutoff frequency of *LP* and *HP* should be such that

$$\kappa_c \leq \frac{1}{2\Lambda}. \tag{3}$$

Finally, the axial resolution of HiLo can be significantly increased by applying a band-pass filter as

$$W(\vec{\kappa}) = \exp\left(-\frac{|\kappa|^2}{2\sigma_w^2}\right) - \exp\left(-\frac{|\kappa|^2}{\sigma_w^2}\right) \tag{4}$$

to the speckle-illuminated image before computing $\langle \sigma_S \rangle_\Lambda$. In fact, the axial resolution can be tuned by changing the parameter σ_w and setting κ_c to approximately $0.18\sigma_w$ [3].

3. Speckle contrast and image quality

From Eq. (2) it follows that the local speckle contrast C_S determines the characteristics of the final image i_{HiLo} and the whole methodology relies heavily on accurately measuring and processing such speckle contrast. Under certain conditions, undesired features of the speckle contrast induce artifacts in i_{HiLo} so that local brightness and particle density measurements can become biased.

The local contrast of speckle patterns presents a typical variation that is inherent to its random nature. For example, if a thin uniform object is imaged using fully developed speckle illumination, the contrast at the sample is approximately 1. However, due to the inevitable filtering caused by the imaging optics, the observed contrast at the camera plane takes an overall value that is significantly lower than 1. The local contrast C_S computed in small regions randomly changes from one region to another and, in fact, it is distributed according to log-normal statistics [8]. As a result, even for uniform samples, the contrast is not uniform throughout the visual field and an artifact is propagated to the final image; regions of high contrast appear brighter than regions of low contrast. As stated by Duncan et al. [8], the

#148475 - $15.00 USD Received 1 Jun 2011; revised 30 Jun 2011; accepted 5 Jul 2011; published 13 Jul 2011

dispersion of the local contrast depends on the side Λ of the sampling window and on the characteristic width of the speckle grains (Δg). However, as it will be shown below, the parameter that determines the dispersion of the local contrast is the ratio $\Lambda/\Delta g$, which represents the square root of the number of speckle grains that fit in each sampling window.

Considering that speckle grains are diffraction limited at the sample, their size in the image plane is approximately determined by the convolution of the illumination and detection squared point spread functions. As an approximation we define $\Delta g \sim 1.22\,\lambda / NA$, where λ is the emission wavelength and NA is the numerical aperture of the microscope objective. The fact that $\kappa_{max} = 2\,NA / \lambda$ is the maximum spatial frequency allowed by the microscope optics, and that κ_c was chosen equal to $1/2\Lambda$ (see Eq. (3)), the ratio $\Lambda/\Delta g$ is related with the cutoff frequency κ_c, according to

$$\frac{\Lambda}{\Delta g} 4.88 \sim \frac{\kappa_{\max}}{\kappa_c}. \tag{5}$$

As the dispersion of contrast values is determined by the ratio $\Lambda/\Delta g$, Eq. (5) indicates that such artifact can be smoothed by properly choosing the value of κ_c. A thorough selection of these parameters is key to assure a good image quality and a satisfactory outcome.

We analyzed this effect using both experimental data and numerical simulations. We defined a "roughness" parameter R calculated as the standard deviation of C_S within the whole image, expressed as a percentage of its mean value $\langle C_S \rangle$, i.e.

$$R(C_S) = \frac{\sigma(C_S)}{\langle C_S \rangle} \times 100 \tag{6}$$

and we numerically analyzed how R depends on the sampling window size (Λ). To do that, a planar uniform object $(\vec{\kappa} = 0)$, illuminated with fully developed speckle of characteristic size Δg = 1.5μm (λ = 0.5μm, NA = 0.4) was synthesized. Speckle illumination was simulated using the Fresnel diffraction theory of coherent light using real parameters of the system and image formation in the CCD was computed using incoherent propagation theory [5, 9].

In Fig. 1(b), we show the roughness R of the image calculated as a function of Λ. The ratio $\Lambda/\Delta g$ is displayed in the top scale while the bottom scale shows $|\kappa_c|/|\kappa_{max}|$, as determined by Eq. (5). For each value of $\Lambda/\Delta g$, 10^4 non-overlapping regions were computed and the same simulation was repeated using speckle grains corresponding to different NA objectives (0.75 and 0.95), showing that the ratio $\Lambda/\Delta g$ is the right parameter to describe R.

This result indicates that to minimize this artifact, in which intensity variations that are not originated in the sample arise, the number of speckle grains within the sampling window should be increased. Nevertheless, if Λ is increased, $|\kappa_c|$ is reduced and consequently the axial resolution decreases. More specifically, since the axial resolution of HiLo heavily relies on processing the LO components using structured illumination, as $|\kappa_c|$ is reduced HiLo approaches the behavior of a wide-field microscope. Alternatively, if speckle grains are shrunk by increasing the NA of the objective, lateral resolution is also improved, but field of view (FOV) is reduced. Given that lateral resolution in HiLo microscopy is independent of $|\kappa_c|$ (it is only limited by diffraction), for admissible values of image roughness, the trade-off to consider is between axial resolution and FOV.

In order to reproduce these results experimentally, we have built a HiLo setup, where the speckle illumination was implemented through the lamp port of an inverted microscope using a ground glass diffuser, a blue diode laser and a lens [1,7], as depicted in Fig. 1(a). The position of the diffuser was conjugated to the back-focal-plane of the objective and uniform illumination images were obtained by rotating the diffuser with a DC motor.

#148475 - $15.00 USD Received 1 Jun 2011; revised 30 Jun 2011; accepted 5 Jul 2011; published 13 Jul 2011

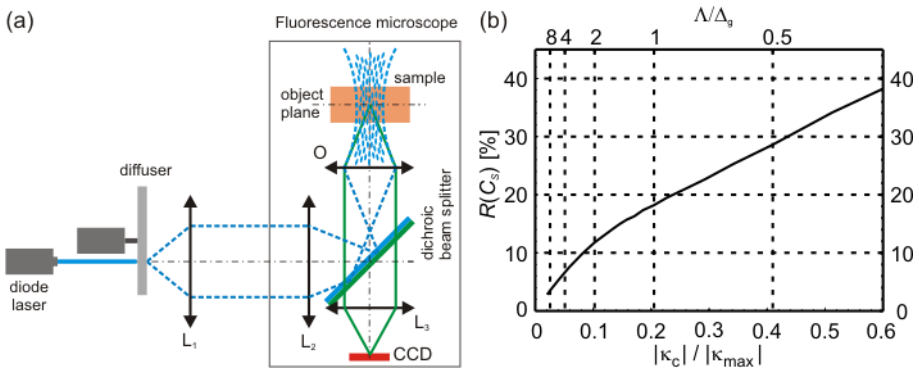

Fig. 1. (a) Scheme of HiLo microscope. A laser diode at 473nm (Laserglow, Toronto, CA) illuminates a ground glass diffuser. Two lenses L_1 and L_2 of 100mm and 300mm focal lengths are used to illuminate the back-focal-plane of an objective in an inverted fluorescence microscope. A CCD camera (Retiga 2000R) was used for imaging. (b) Output roughness as a function of $|\kappa_c|/|\kappa_{max}|$ (bottom axis). The parameter $\Lambda/\Delta g$, in the top axis, roughly represents the square root of the number of speckle grains that fits in each sampling window.

We fabricated a sample consisting of several squared monolayers of fluorescent proteins of 20×20 μm^2 using a method that allows printing protein patterns of arbitrary shapes and concentrations with micron resolution [10, 11]. For our experiments we produced squared uniform distributions of Avidin-Fluorescein and the sample was imaged using a 60X 1.35*NA* objective.

HiLo images of the same fluorescent pattern obtained with different values of Λ and a standard widefield image are displayed in the four panels of Fig. 2(a). As can be observed, the roughness artifact is efficiently smoothed by increasing Λ without distorting lateral resolution. Furthermore, in Fig. 2(b) intensity profiles of the images displayed in Fig. 2(a) are traced, where the reduction of the artifact is also evident. For quantifying this effect, the experimental roughness within the central region (15×15μm^2) of the image, was computed on i_{HiLo} similarly to Eq. (6). The values of $R(i_{HiLo})$ are plotted in Fig. 2(c) for different sizes of the window, showing that it strongly depends on $\Lambda/\Delta g$ as calculated with numerical simulations in Fig. 1(b).

This effect must be taken into consideration when planning biological imaging. It is not problematic for 3-dimensional reconstructions, image segmentation, fluorescence recovery after photobleaching, measuring fluorescent protein expression levels, etc. Nevertheless, for single particle tracking, image correlation spectroscopy or colocalization studies, it must be taken into account.

#148475 - $15.00 USD Received 1 Jun 2011; revised 30 Jun 2011; accepted 5 Jul 2011; published 13 Jul 2011

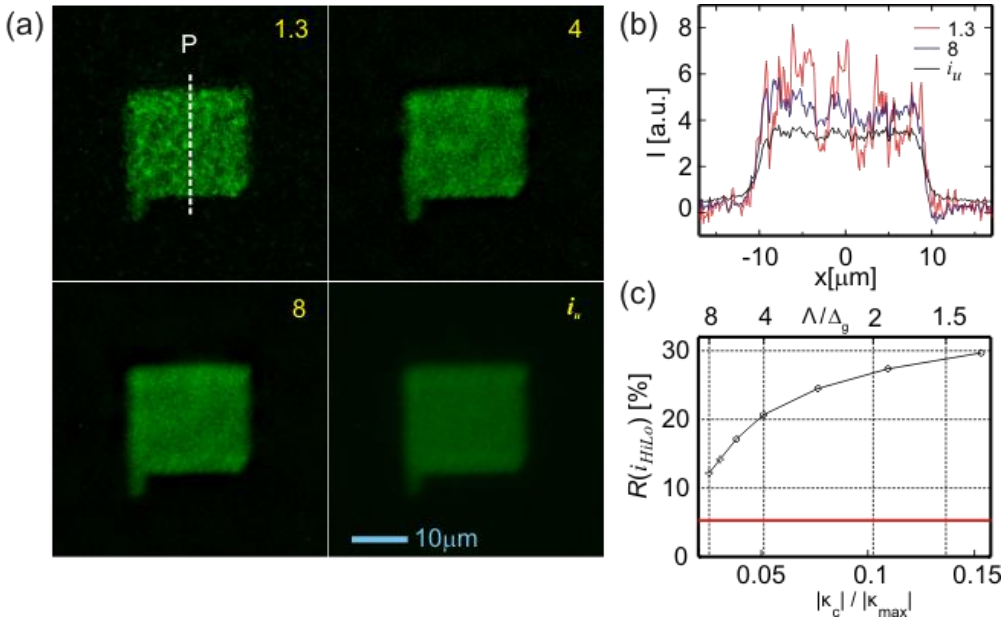

Fig. 2. 20×20μm2 planar object imaged in-focus with a 60X NA=1.35 objective. (a) HiLo Images obtained using sampling windows with Λ/Δg of 1.3, 4 and 8 as indicated. In the experiment Δg = 0.46μm. The image obtained with uniform illumination is also shown. (b) Intensity profiles of images in (a) traced over the vertical dashed line P. (c) Roughness of the experimental image for various values of *Λ/Δg* (upper scale). The corresponding values of $|\kappa_c|/|\kappa_{max}|$ are shown in the bottom scale. The dashed red line represents the roughness of i_u.

4. Speckle contrast and optical sectioning

A second issue we considered is the situation of thick objects. In these cases, the out-of-focus fluorescence can be high enough to change the speckle contrast yielding non-intuitive results. On one hand, when the fluorescence background is very intense, the contrast is deeply reduced. In conditions in which speckle contrast is so low that cannot be distinguished from noise, *Cs* becomes a flat function that doesn't discriminate signal from background. On the other hand, strong fluctuations in the object thickness, produce fluctuations in *Cs* that propagate to the final HiLo image showing an artificial variation of the intensity, which does not reflect a change of fluorophore concentration inherent to the optical section imaged. As opposed to confocal laser scanning and multiphoton microscopies, which measure fluorescence signals that originate only at in-focus plane, HiLo uses information that arises from out-of-focus regions too, and this fact must be considered in the analysis. As the out-of-focus fluorescence affect the image contrast, this effect is not specific to speckle illumination and could be generalized to other structured illumination approaches that rely on the analysis of the contrast to obtain optical sectioning. However, the specific impact on each particular technique should be separately studied.

The out of focus sections of the sample produce a fluorescence background that ultimately affects HiLo images in a non-intuitive way. Speckle illumination consists of a pattern of grains in which size remains relatively constant along the propagation direction of the beam, as depicted in Fig. 1(a). Therefore, when a fluorescent object thicker than the focal volume is illuminated like this, the epi-fluorescence detected combines the signal originating from speckle grains located at different depths. While speckle grains near the object plane yield high contrast, the grains located off-plane produce a defocused background that lessens the values of Cs.

Summarizing, an increase in out-of-focus fluorescence background produces an overall decrease of *Cs*, since off-plane fluorescence contributes low speckle fluctuations but increases

#148475 - $15.00 USD Received 1 Jun 2011; revised 30 Jun 2011; accepted 5 Jul 2011; published 13 Jul 2011

the total signal. In fact, *Cs* acts as a weighting function that highlights the signal originated from the in-focus regions over those out-of-focus, but the strength of such enhancement becomes limited when C_S is too small. Even in the absence of speckle, acquisition noise (shot noise, readout noise, etc) produces an intensity contrast (C_N). Albeit the mean value of C_N can be numerically reduced to zero [1,3], the fluctuations around the mean cannot be avoided and when, in strong background conditions, the speckle fluctuations are minimized, the capacity to distinguish in-focus from out-of-focus information is lost. When speckle fluctuations originated from in-focus regions become similar to noise, optical sections cannot be obtained, and this effect ultimately imposes a limit to the characteristics of objects that can be analyzed using HiLo microscopy.

In order to study the dependence of contrast on the axial thickness of the sample in more detail, we combined experimental data and numerical simulations, as described above. We first computed numerically the illumination pattern produced by a diffuser to show the 3D structure of speckle grains and three examples at different depths are shown in Fig. 3(a). To simulate the speckle illumination image produced by a thick fluorescent object in the CDD, we calculated the incoherent propagation of all object planes at different depths to the detector. The final image was obtained by summing up all such propagated intensities. This procedure was repeated for samples of different thicknesses and in each case the overall contrast was computed in the central region of the final image. The curves in Fig. 3(b) represent the simulated contrast versus the axial thickness *T* of the sample, where each line corresponds to a different *NA* objective.

Experimentally, we tested this effect by fabricating a fluorescent sample of variable thickness as depicted in Fig. 3(c). It consists of a wedge-shaped glass chamber made with coverslips and filled with a fluorescent dye solution (fluorescein in water and 10% methanol). Objects of different thicknesses were obtained by simply moving transversally the sample with respect to the microscope objective. At each position on the sample, the thickness was measured using a homemade Fourier-domain optical coherent tomography device coupled to the lateral port of the microscope [12, 13]. The contrast obtained for each position is plotted with discrete markers in Fig. 3(b) and a good match between the experiments and numerical simulation can be observed (a 1.4 scaling factor was used).

As shown in Fig. 3(b), for a given sample thickness, the contrast is higher for low *NA* objectives. The reason for this is that when objects are illuminated with high *NA* objectives, speckle grains are small, the Rayleigh range is narrow, and therefore the fraction of out-of-focus fluorescence measured is high. To mitigate this effect, the size of speckle grains must be increased, which can be achieved by reducing the *NA* of the objective. In this case, a trade-off between the sample width and the lateral resolution should be considered. An alternative approach is to reduce only the NA of the illumination. This could be done by placing an iris in the illumination pathway but not in the detection pathway (i.e. before the dichroic beam-splitter). Thereby, the size of the grains is increased without compromising lateral resolution but reducing the FOV; there is a trade-off between sample width and FOV.

As stated above, HiLo images depend on *Cs*, but more specifically on the product of *Cs* and i_u (see Eq. (2)). If we consider the sample depicted in Fig. 3, we expect an optical section to render a constant intensity image, since the dye concentration is homogeneous at any depth. The value of *Cs* is reduced as the axial thickness of the sample increases, but the widefield intensity i_u increases. However, it is not clear if these variations would compensate, and in general whether the HiLo image is uniform.

#148475 - $15.00 USD Received 1 Jun 2011; revised 30 Jun 2011; accepted 5 Jul 2011; published 13 Jul 2011

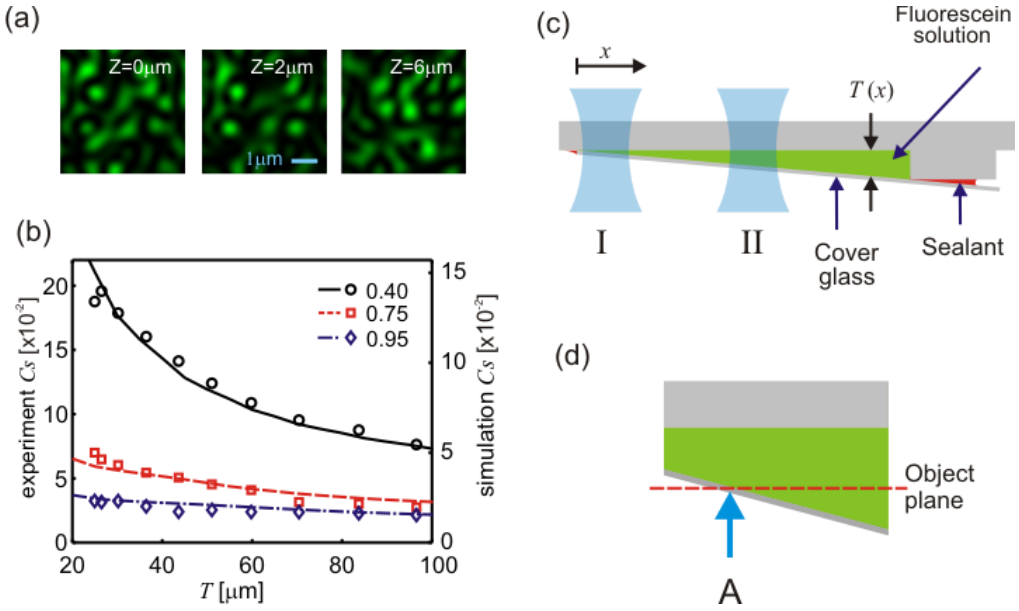

Fig. 3. (a) Numerical simulation of speckle produced with λ = 488 nm and NA=0.4 in 3 axial planes. (b) Contrast of speckle illuminated sample (c) at various axial widths. Each position of the sample was illuminated with objectives of 3 different NA. The discrete markers correspond to the experimental measurements while the lines represent numerical simulations. Estimated experimental uncertainties are smaller than the markers size. Note that experiment and numerical simulation results are plotted with different scales. (c) Scheme of wedge-shaped glass chamber filled with fluorescent solution. The sample was imaged in regions I and II. (d) Scheme depicting the position of the object plane in a region of sample in (c).

To experimentally illustrate this situation, we fabricated samples like the ones in Fig. 3(c) having large angles to obtain substantial variations of the thickness within the FOV. Two regions of the sample (I and II) were measured as indicated in the figure. The total thickness variation within the FOV is approximately the same (40μm) in both regions, but the mean thickness in region I is 40μm and in region II is 160μm. The corresponding experimental results are presented in Fig. 4. The top plots on the right column show i_u vs. $T(x)$ along with their linear fits. In both cases, the intercepts of both linear fits are approximately 0, consistent with the fact that the intensity vanishes as T→0. For each region, the images corresponding to i_s, i_u, Cs and i_{HiLo} are presented in the left, and the averaged horizontal profiles are plotted with black markers on the right.

The results show that the changes on Cs and i_u, due to variations in the out-of-focus background, do propagate to the final i_{HiLo} image yielding optical sections of non-constant intensities. These variations are more dramatic in region I, where Cs decreases so steeply with T that the linear increase of i_u is clearly not enough to compensate for it. Besides, in the graph of i_{HiLo} for region I, a local maximum can be observed near x=100μm. This point (A) corresponds to the position where the object in-focus plane intercepts the edge of the sample, as schematized in Fig. 3(d), and for x<A, $Cs(x)$ decreases as the object gets out of focus, while for x>A a part of the object is in focus, but Cs(x) decreases as the object thickness increases. Indeed, the Cs peak shifts accordingly in x, as the object plane is axially displaced (data not shown), confirming this explanation.

In region II, the variation in $Cs(x)$ is smaller than in Region I, so that it is approximately compensated by the increase in i_u yielding a rather uniform i_{HiLo} optical section. Interestingly, the total thickness change in regions I and II is the same (40μm), but the effects of the relative variation ΔT/T in Cs and i_u are not inversely proportional.

#148475 - $15.00 USD Received 1 Jun 2011; revised 30 Jun 2011; accepted 5 Jul 2011; published 13 Jul 2011

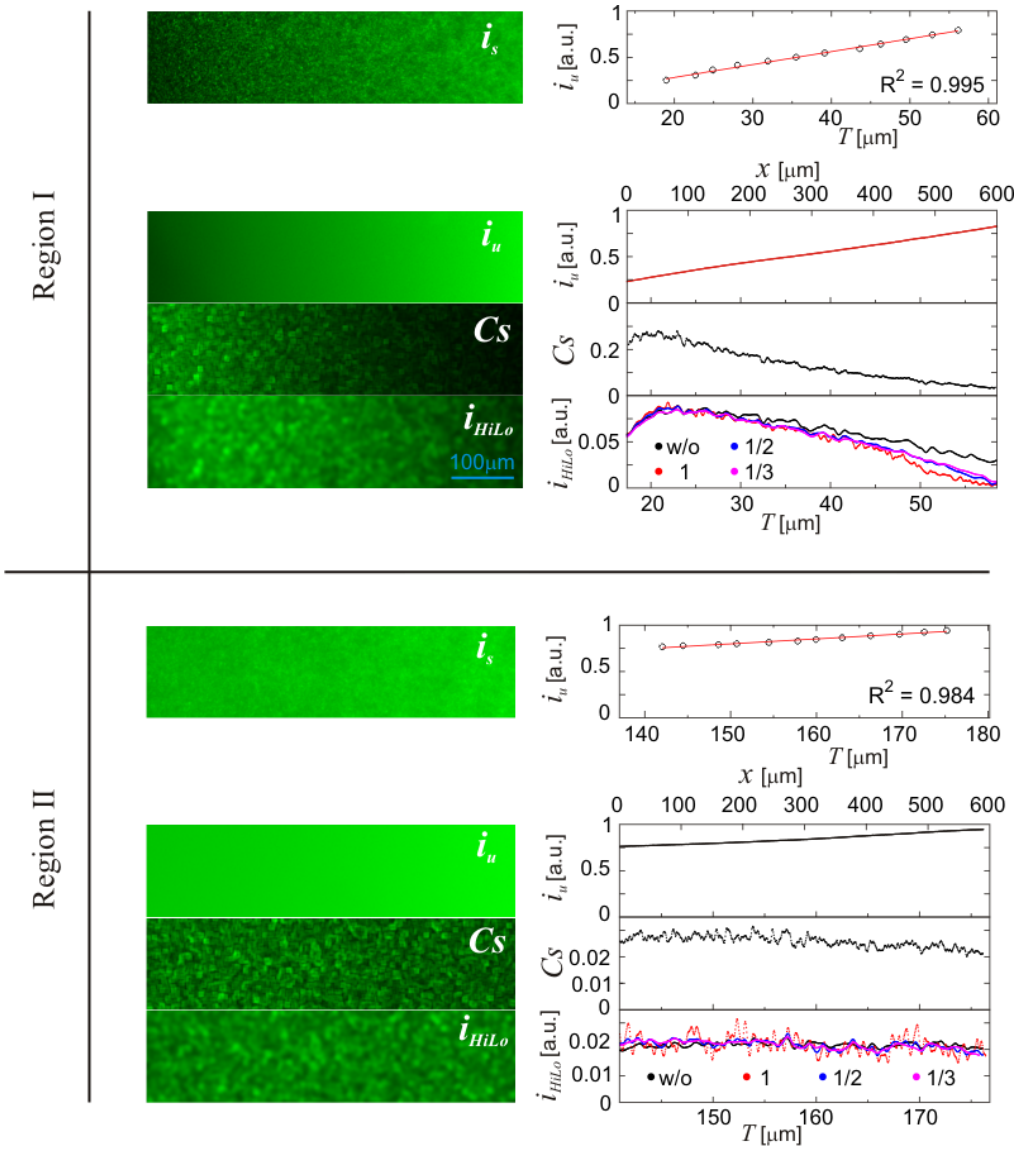

Fig. 4. Images of a wedge-shaped chamber filled with dye solution in two regions: I is a thin region of main thickness ~40μm and II is a thicker region of main thickness ~160μm. Each panel is organized as follows: In the left column the images i_s, i_u, *Cs* and i_{HiLo} are shown while the three bottom plots in the right column show the corresponding average horizontal profiles (notice the transversal coordinate is displayed in the top scale and the bottom scale indicates thickness of the sample). The profiles of i_{HiLo} including band-pass prefiltering with $\sigma_w=\kappa_{max}$, $\kappa_{max}/2$ and $\kappa_{max}/3$ are displayed (with independent normalization factors) along with i_{HiLo} obtained without prefiltering. The top graph of each right column shows the linear fit of i_u vs. the thickness T demonstrating the linearity of the CCD in the measured range. i_{HiLo} without band-pass filter was computed with Λ=11 pixels, and $|\kappa_c|=1/2\Lambda$. The objective is a 10X 0.4NA, and the CCD pixel size is 7.4 μm.

We finally computed i_{HiLo} using the pass-band filter of Eq. (4) to assess its impact on the effect described above. The intensity profiles obtained with filters built with $\sigma_w=\kappa_{max}$, $\kappa_{max}/2$ and $\kappa_{max}/3$ are plotted in the bottom graphs of Fig. 4 along with the result without prefiltering, showing that this operation does not change the overall behavior regarding the non-constant intensity profiles produced by background fluctuations.

#148475 - $15.00 USD Received 1 Jun 2011; revised 30 Jun 2011; accepted 5 Jul 2011; published 13 Jul 2011

Overall, in contrast to what happens in confocal microscopy, since in-focus and out-of-focus fluorescence are used to calculate the optical sections, this combination needs to be understood for a correct interpretation of the HiLo images. The profile of the optical sections obtained with both techniques can be different and this fact must be considered.

It is worth mentioning, however, that typical biological samples are seldom as ubiquitously fluorescent as a dye solution. In consequence, in most cases the out of focus background will not produce such a dramatic effect. Nevertheless, if precise quantifications of the intensity are sought, this effect should be acknowledged.

5. Conclusions

Speckle contrast measurement and processing is key for obtaining optimum results with HiLo microscopy. In this work we have studied two aspects that determine the characteristics of HiLo images. Firstly, we have shown that artificial roughness due to speckle illumination can propagate to the final image and that this artifact can be smoothed by properly choosing the number of speckle grains that fit in the sampling window used for computing the contrast. The size of the grains and such computation ultimately implies a trade-off between axial resolution and field of view of the final image. Secondly, thick fluorescent objects can reduce speckle contrast, hampering the ability to reject out-of-focus fluorescence and yielding optical sections that differ from those traditionally obtained with laser scanning microscopies. In this situation, contrast can be improved by reducing the *NA* in the illumination pathway, which yields a compromise between the sample width and the filed of view.

HiLo microscopy is a very promising technology that provides optical sectioning and fast acquisition at a low cost. The results presented here can be used as a guide to adjust its different parameters for obtaining optimal imaging.

Acknowledgments

This work was funded by grants from the Fondation de l'Hôpital Maisonneuve-Rosemont (La néphrologie et son Impact) to SC and SL, the National Sciences and Engineering Research Council (NSERC) and the Fonds Québécois de la Recherche sur la Nature et les Technologies (FQRNT) grants to SC. SC and SL are recipients of a salary awards from Fonds de la Recherche en Santé du Quebec (FRSQ). JM and DK are recipients of HMR postdoctoral fellowships, JMB from NSERC and KS from FRSQ.

#148475 - $15.00 USD Received 1 Jun 2011; revised 30 Jun 2011; accepted 5 Jul 2011; published 13 Jul 2011